1982

Measurement of Operating Conditions of Rolling Piston Type Rotary Compressors

E. Sakurai

J. F. Hamilton

MEASUREMENT OF OPERATING CONDITIONS OF ROLLING PISTON TYPE ROTARY COMPRESSORS

EISUKE SAKURAI
MAJOR APPLIANCE PRODUCTS
ENGINEERING LABORATORY
TOSHIBA CORPORATION
4-1, UKISHIMA-CHO
KAWASAKI-KU, KAWASAKI 210
JAPAN

JAMES F. HAMILTON, PROFESSOR
THE R. W. HERRICK LABORATORIES
PURDUE UNIVERSITY
WEST LAFAYETTE
INDIANA 47907
USA

ABSTRACT

A rolling piston type rotary compressor was modified for measurement of dynamic pressures in the compression and suction chambers, and instantaneous angular position of the shaft. The compressor connected with a compressor load stand was tested at three different loads by changing discharge gas pressure and different running speeds by controlling line frequency between 35 to 75 herts. The analog data on pressures and angular position of the shaft was converted into digital data at the local site and processed at the remote site for plotting P-V diagrams and angular position shift curves. Indicated gas work, frictional loss, and mechanical and indicated efficiencies were obtained with high accuracy, based on the P-V diagram.

The results show that mechanical and indicated efficiencies at higher running speeds are less than at lower speeds, over operation speed between 35 to 75 hertz. The shaft does not rotate at constant speed during one cycle, particularly under operation at low frequency. The fluctuation of the speed of the shaft increases as the average shaft speed decreases.

INTRODUCTION

Controlling cooling or heating capacity of an air conditioner with a variable-speed compressor becomes popular recently as one of the most effective ways to improve SEER of the air conditioner. As inexpensive, highly reliable power semiconductors have been developed, even household air conditioners begin to be equipped with frequency convertors using the semiconductors to control running speeds of induction motors in the refrigerant compressors. A rolling piston type rotary compressor combined with the frequency convertor may be suitable for a small-sized air conditoner requiring a wide control range in capacity because high volumetric efficiency may be kept constant for the rotary compressors, unlike reciprocating compressors, as the running speed becomes higher.

A rolling piston type rotary compressor designed for constant-speed operation was picked up and then modified for investigating operating conditions over wide speed range under various load. The compressor with a two-pole, single-phase induction motor was operated at various rotational shaft speeds between 1880 to 4390 rpm by changing the input frequency between 35 to 75 herts. Three different loads were applied on the compressor by changing discharge gas pressure.

Two kinds of measurements of the operating conditions will be presented mainly in this paper; measurement of P-V (pressure-volume) diagrams, which is fundamental to analyze thermodynamic losses of the compressor, and measurement of shaft speed fluctuation in one cycle, which is related to the accuracy of the measurement of P-V diagrams.

EXPERIMENTAL PRINCIPLES

P-V diagrams

The measurement of P-V diagrams was done as precisely as possible. The following are basic concepts of the methods for measuring the diagrams.

(1) measurement of instantaneous angular position of the shaft in rotation, not to be affected by the revolving flutter due to the change of the load in one cycle

(2) accurate conversion of the angular position measured to the cylinder volume, depending on basic equations which express the geometric relationship between volume and angular position

(3) accurate calculation of the area of the P-V diagram

In order to make the methods above possible digital computers for sampling and process-

ing data was used in the measurement system. The conversion from angular position to cylinder volume, and the calculation of the area of the P-V diagram were carried out by using geometric equations [1] and trapezoidal rule respectively programmed in the computer.

Instantaneous shaft speed

Instantaneous angular position of the rotating shaft was measured by using two sensors for detecting reference angular position and counting the number of regular angular intervals. There were two different ways to utilize the signal from the second sensor: for measuring P-V diagrams and instantaneous shaft speeds. While the cylinder pressures were sampled with an A-D convertor at every constant angular interval detected, for the P-V diagram, the signal of constant angular interval was sampled at every constant time interval for the measurement of instantaneous shaft speed. Instantaneous shaft speed was obtained by differentiating the data of angular interval with respect to time numerically with the computer.

EXPERIMENTAL APPARATUS

Test compressor

An existing rolling piston type rotary compressor with a displacement volume of 10.3 cc per revolution was modified for measurement of the dynamic pressures in the compression and suction chambers, and the instantaneous angular position of the shaft. Cross-sections of the compressor are shown in Figure 1 and 2. The existing shell of the compressor was replaced with the bolted shell designed for the installation of transducers, a timing gear, cable connectors, etc.

Operation of compressor

The compressor for the test was connected to a hot gas load stand, similar to the one shown in reference [2]. The stand was equipped with an orifice system for measuring mass flow rate. Three different loads, as shown in Table 1, were applied on the compressor by changing the discharge gas pressure. The frequency of power source was changed with a frequency convertor which consisted of an AC-DC convertor, a DC motor, and an AC generator. The frequency range was limited to 35 to 75 herts due to the limitation of the frequency generated by the convertor while the compressor might run properly out of the frequency range. To make the induction motor of the compressor drive most efficiently at various frequencies, the voltage supplied was changed so as to have a constant value which is ratio of voltage to frequency. From some preliminary experiments, the ratio was determined to be maintained at 2.0 volt per hert.

Dynamic pressure measurement

Three piezoelectric pressure transducers were used for measuring the dynamic pressures in the cylinder as shown in Figure 4. Since the compression and suction processes occur simultaneously in different chambers in rolling piston type compressors, at least two pressure transducers were required in the suction and compression chambers respectively to obtain P-V diagrams. These two pressure transducers were mounted near the suction port and the discharge port respectively. A third pressure transducer was mounted between these two so that it may measure the pressure of either the suction or compression process. The pressure measured with the third transducer was used as a reference pressure to determine relative pressure level between the two dynamic pressures.

All of the three pressure transducers were recessed as shown in Figure 3. With the recessed mount, the pressure at the point desired can be measured without interrupting other functions of the compressor. The recessed mount may cause gas dynamic due to the contained volume of the adapter system [3,4], contamination of the measurement by these dynamic effects is avoidable by proper adjustment of the contained volume.

Calibration of the pressure transducers was carried out prior to installing them in the compressor. The calibration includes both the pressure sensitivity and the static temperature sensitivity as discussed in reference [5,6].

Angular position measurement

A measurement system composed of two proximitor probes and a timing gear, was utilized to provide accurate data concerning the angular position of the shaft in the presence of rotational speed fluctuations. The arrangement of the probes and the gear on the upper side of the motor is shown in Figure 1 and 5. A gear with 178 teeth was selected to obtain high resolution of the angular position. One of the two probes was set horizontally as close to the gear as possible so as to recognize each tooth clearly. The other one was set vertically as to detect a notch on the upper side of the gear. The notch location corresponded to the top dead center as a reference angular position.

SIGNAL PROCESSING

Signal processing for P-V diagrams

The signal processing for P-V diagrams may be separated into two major ones: processing analog data to digital at a local site, and processing the digital data to draw and integrate P-V diagrams at a remote site.

The signal conditioning process at the local site is shown in Figure 6. The sampling interval of the pressure signal in the A-D convertor was controlled by an external clock terminal using the signal from the proximitor probe facing at the gear teeth. Since the number of the gear teeth was 178, each sampling for pressure should occur at every 2.02 deg.. The signal from the proximitor probe detecting the reference angular position of the top dead center was used as an external trigger source to start sampling. The wave form of the trigger source was also sampled after triggering occurred. The signal of the trigger source sampled was used for obtaining not only the initial angular position when the triggering took place, but also the average rotational speed of the shaft so that an internal clock worked to generate constant sampling time-interval for this sampling. Each signal was independently sampled, averaged over fifty times, and then punched out on paper tape.

The paper tape then processed with a large-scale digital computer. The flow chart for the processing is shown in Figure 7. The rotational speed of the shaft, n_s, is

$$n_s = \frac{1}{T} = \frac{1}{(i-j)\Delta t - m\Delta t + n\Delta t} \quad (1)$$

From an interpolation of the assumed parabolic curve for the local voltage-time history around a peak shown in Figure 8, the two peak locations are found

$$m = \frac{E(i-1)-E(i+1)}{2[E(i+1)-2E(i)+E(i-1)]} \quad (2)$$

$$n = \frac{E(j-1)-E(j+1)}{2[E(j+1)-2E(j)+E(j-1)]} \quad (3)$$

The initial angular position, θ_i, at which the triggering occurs in advance of the first peak of the top dead center is then

$$\theta_i \doteq \frac{360\Delta t\ (1-i-m)}{T} \quad (4)$$

The angular position of each pressure sample specified with the number of sampling order, k ($k \geq 1$), is

$$\theta = \frac{360(k-1)}{N_G} + \theta_i \quad (5)$$

Finally the volumes of the suction and compression chambers are determined as a function of the shaft angular position using the geometric equations in reference [1] .

Determination of absolute pressure levels for the two major dynamic pressures in suction and compression chambers was carried out as shown in Table 2, basing on the third dynamic pressure, P_M, and static suction gas pressure, P_e. The three areas in P-V diagram which correspond to effective gas work, We, oversuction loss, l_s, and overcompression loss, l_c, are respectively

$$w_n = \int_{\theta_1}^{\theta_2}(P_c-P_e)dV_c + (P_d-P_e)\int_{\theta_2}^{\theta_3}dV_c \quad (6)$$

$$l_s = \int_{\theta_1}^{\theta_3}(P_e-P_s)dV_s \quad (7)$$

$$l_c = \int_{\theta_2}^{\theta_3}(P_c-P_d)dV_c \quad (8)$$

where θ_1: angular position at which the compressin process starts (=32°)
θ_2: angular position at which P_c starts to exceed P_d
θ_3: angular position at which the discharge process finishes (=339°)

During the transitional range from θ_3 to θ_1 no gas work by the rotating motion of the shaft is necessary since the suction chamber is connected to the compression chamber. Reexpansion process of the trapped gas in the additional volume including the volume of discharge port occurs during this range, however, thermodynamic loss of the reexpansion is not defined on this paper because reexpansion loss may be obtained with not only the P-V diagram but also the data on thermodynamic mixing process in the single chamber and inverse flow through the suction port that were not measured. Therefore, indicated gas work, w_i, and indicated efficiency, η_i, are defined as

$$w_i = w_n + l_s + l_c \quad (9)$$

$$\eta_i = w_n/w_i \quad (10)$$

The indicated frictional loss, W_f, and the mechanical efficiency, η_{me}, are finally

$$W_f = W_{mo}\eta_{mo} - n_s w_i \quad (11)$$

$$\eta_{me} = (n_s w_i)/(W_{mo}\eta_{mo}) \quad (12)$$

where the motor input power, W_{mo}, was measured and the motor efficiency, η_{mo}, was provided from the compressor manufacturer.

Signal processing for instantaneous shaft speed

The instrumentation used for obtaining the indicated gas work was also available for measuring instantaneous shaft speed, however, processing the signal from the detector facing the gear teeth was different after the signal conditioning with the AC amplifier. The signal was sampled with constant sampling time-interval with the A-D convertor at local site. The samples were connected again with straight lines in order with another computer at the remote site. The time period, T_k, corresponding one gear tooth or one angle interval (2.02 degree), as shown in Figure 9 can be predicted:

$$T_k = \Delta t \frac{-E(j)}{E(j-1)-E(j)} - \Delta t \frac{-E(i)}{E(i-1)-E(i)} + (j-i-1)\Delta t \quad (13)$$

The instantaneous shaft speed, n_i, during time period specified, T_k is

$$n_i = 1/(N_G T_k) \quad (14)$$

The time period for one rotation of the shaft, T, and the average shaft speed, n_s, are

$$T = \sum_{k=1}^{N_G} T_k \quad (15)$$

$$n_s = 1/T \quad (16)$$

Therefore, the fluctuation of the shaft speed, D, is

$$D = (n_i/n_s) - 1 \quad (17)$$

Angular Position shift, $\Delta\theta$, is the difference between the actual angular position and the ideal angular shaft position with an assumption of constant rotational speed equal to the average speed, n_s, as shown in Figure 10. The angular position shift is

$$\Delta\theta = 360 \left(\frac{N}{N_G} - \frac{1}{T} \sum_{k=1}^{N} T_k\right) \quad (18)$$

where N is the order number of the gear teeth after the triggering with the A-D convertor occurs by the signal of the reference angular position.

RESULTS AND DISCUSSIONS

Losses and efficiencies from P-V diagrams

Two sets of three P-V diagrams plotted with the computer are shown in Figure 11 and 12. As the frequency increases, Figure 11 shows that overcompression and oversuction losses become larger due to increasing of mass flow rate which was observed to be almost proportional to the frequency, as shown in Figure 17. On the other hand, the oversuction or overcompression losses at the three differnt loads do not differ from one loss to another since the mass flow rate, as shown in Figure 17, is not affected so much by changing the discharge gas pressure. Frictional losses were obtained as shown in Figure 13. While the frictional loss increases as the frequency increases, the frictional losses at three various loads may be at almost same level compared with the magnitudes of indicated gas power, $w_i n_s$, and motor output power, $\eta_{mo} W_{mo}$, in Figure 13 and 14. Indicated and mechamical efficiencies are shown in Figure 15. The lower indicated efficiency at higher frequency is due to larger overcompession and oversuction losses occurred by higher mass flow rate. Why the indicated efficiency becomes higher, as the load becomes heavier, may be: since the overcompression or oversuction losses at three different loads may be almost at same level, larger effective gas work leads higher indicated efficiency, based on equation (9) and (10). For the difference between mechanical efficiencies at three different loads, the same concept would be applicable; if the frictional loss in the compressor is dominated by fluid lubrication rather than boundary lubrication, the frictional loss may be independent on the load, as reasonably shown in Figure 13. Therefore, if the frictional loss is constant at various loads, larger indicated gas work leads higher mechanical efficiency, based on equation (11) and (12). From looking through Figure 15, 16, and 17, it is found for the rolling piston type rotary compressor, that the indicated and mechanical efficiencies decreases as the rotational shaft speed increases while the mass flow rate increases proportionally to the shaft speed, that is, the volumetric efficiency is kept constant.

Shaft speed fluctuation and angular position shift

Data on running speed fluctuation and angular position shift is shown in Figure 18, 19, and 20. It is apparent from this data that the shaft does not rotate at constant speed during one cycle, particularly under operation at low frequency. The fluctuation of the shaft speed increases as the average shaft speed decreases. For example, using the curve at 35 Hz in Figure 18, when the angular position of the shaft is around 120 degree, it is observed that the shaft rotates 8 percent faster than the average shaft speed. One can observe secondary wave like saw on a fundamental wave like sine wave in Figure 18, however, this saw-wave may be due to the insufficient number of samples; the sampling one time per a quarter of one cycle for one gear tooth, which is necessary at least to remake wave form similar to the original wave, was difficult due to the lacking ablity with the A-D convertor. Then, the curve at 35 Hz in Figure 19 shows that when the cycle time is 0.5 or the ideal angular position under the assumption of constant shaft speed is 180 degree, the actual angular position then is addition of the angular position shift, 7 degrees shown, to the ideal angular position, or 187 degree altogether. Figure 20 shows that the anglar position shift or the shaft speed fluctuation does not differ very much when the compressor load changes. Finally, as an example possible error in the indicated gas work, consider that only the reference angular position is measured, and the P-V diagram is obtained using the assumption that there is no fluctuation about the shaft speed in one cycle. In Figure 21,

the best reference angular position to avoid the error is found to be at 150 to 160 degree for both 50 and 60 Hz.

CONCLUSION

(1) Frictional loss, indicated gas work, and mechanical and indicated efficiencies were investigated experimentally by obtaining P-V diagrams.

(2) The fluctuation of the shaft speed was investigated by using the same measurement system with which the P-V diagram was measured.

(3) The mechanical and indicated efficiencies measured decreases as the rotational shaft speed increases between 1880 to 4390 rpm.

(4) The fluctuation of the shaft speed increases as the average shaft speed decreases.

REFERENCES

1. Pandeya, P., and Soedel, W., "Rolling Piston Type Rotary Compressors with Special Attention to Friction and Leakage", PCTC 1978, p. 209-225.

2. Soedel, W., "Introduction to Computer Simulation of Positive Displacement Type Compressors", Herrick Labs.,1972,

3. Elson, J.P., Soedel, W., "Criteria for the Design of Pressure Transducer Adapter System", PCTC 1972, p. 390-394.

4. Deobelin, O.E., "Measurement System", McGraw-Hill, 1975, p.391

5. Lancaster, D.R., Krieger, B.R., and Lienesh, J.H., "Measurement and Analysis of Engine Pressure Data", SAE Report No. 750026, p. 155-172.

6. Alyea, W.J., Uyehara, A.O., and Myers, S.P., "The Development and Evaluation of an Electric Indicated Horsepower Meter", SAE Report No. 69018, p.784-802.

NOMENCLATURE

n_i	instantaneous shaft speed
n_s	average shaft speed
T	period of one cycle
Δt	constant samping time interval
i,j,k	number of sampling order
m,n	value indicating difference from peak
E	voltage level of signal
θ	angular position of shaft from top dead center to minimum clearance between roller and cylinder wall
θ_i	angular position of the first sample taken
N_G	number of gear teeth
V_c	volume of compression chamber
V_s	volume of suction chamber
P_e	static suction gas pressure
P_d	static discharge gas pressure
P_s	dynamic pressure measured at 20°
P_M	dynamic pressure measured at 160°
P_c	dynamic pressure measured at 340°
W_f	frictional loss
W_{mo}	motor input power
w_i	indicated gas work
w_n	effective gas work
l_c	overcompression loss
l_s	oversuction loss
η_{mo}	motor efficiency
η_i	indicated efficiency
η_{me}	mechanical efficiency

TABLES AND FIGURES

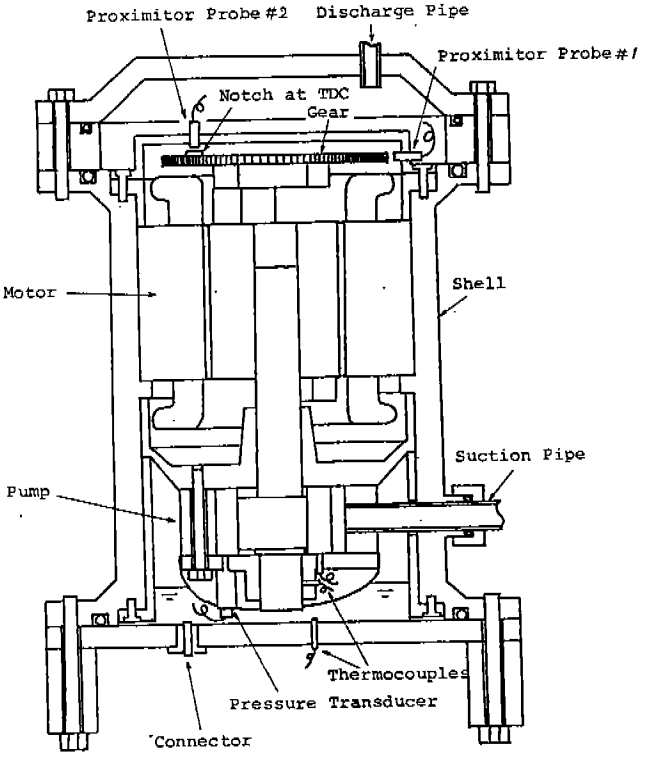

Figure 1 Overall Cross-section of Modified Compressor

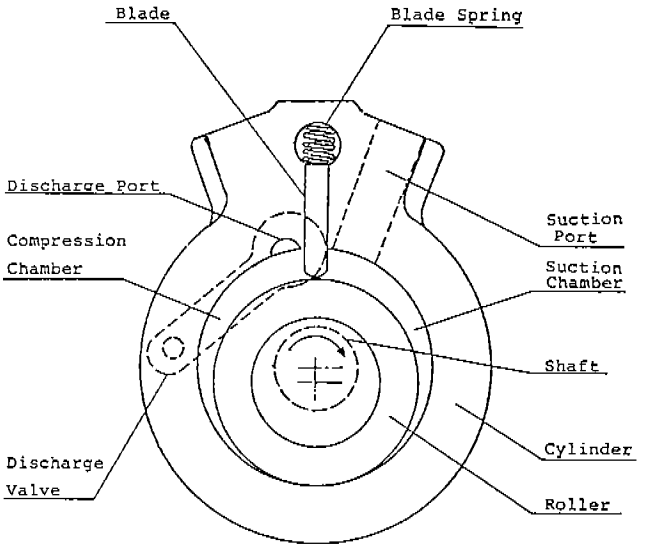

Figure 2 Cross-section of Cylinder Before Mounting Pressure Transducers

Condition	Unit	Load		
		Light	Medium	Heavy
Discharge Gas pressure	MPa	1.77	2.15	2.46
Suction Gas Pressure	MPa	0.627	0.627	0.627
Suction Gas Temperature	°C	35	35	35
Compressor Surface Temperature	°C	75	75	75

Table 1 Cycle Condition

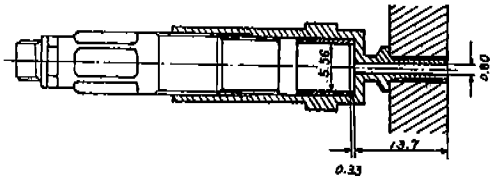

Figure 3 Recessing Mount

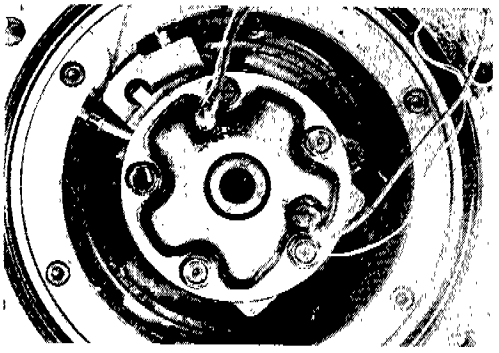

Figure 4 Pressure Transducers Mounted

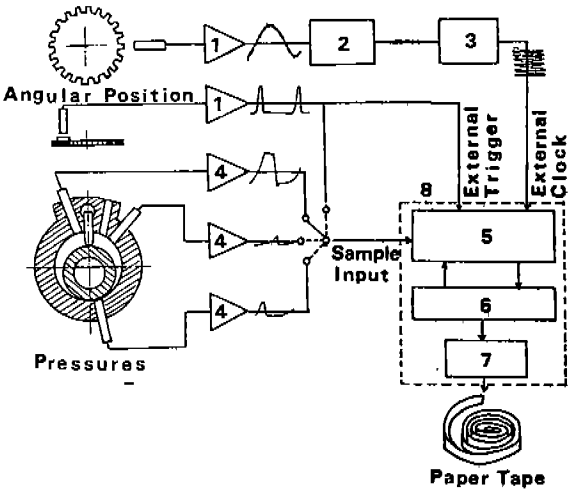

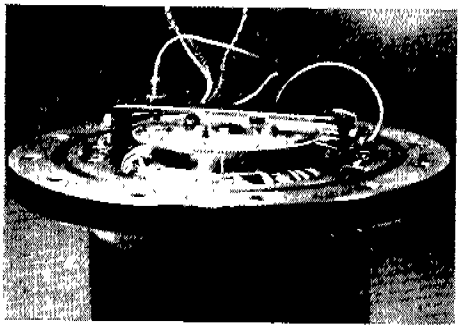

Figure 5 Proximitor Probes and a Gear Mounted

1 Proximitor
2 High Pass Filter
3 AC Amp.
4 Charge Amp.
5 AD Converter
6 Computer
7 Tape Puncher
8 FFT

Figure 6 Measurement System at Local Site

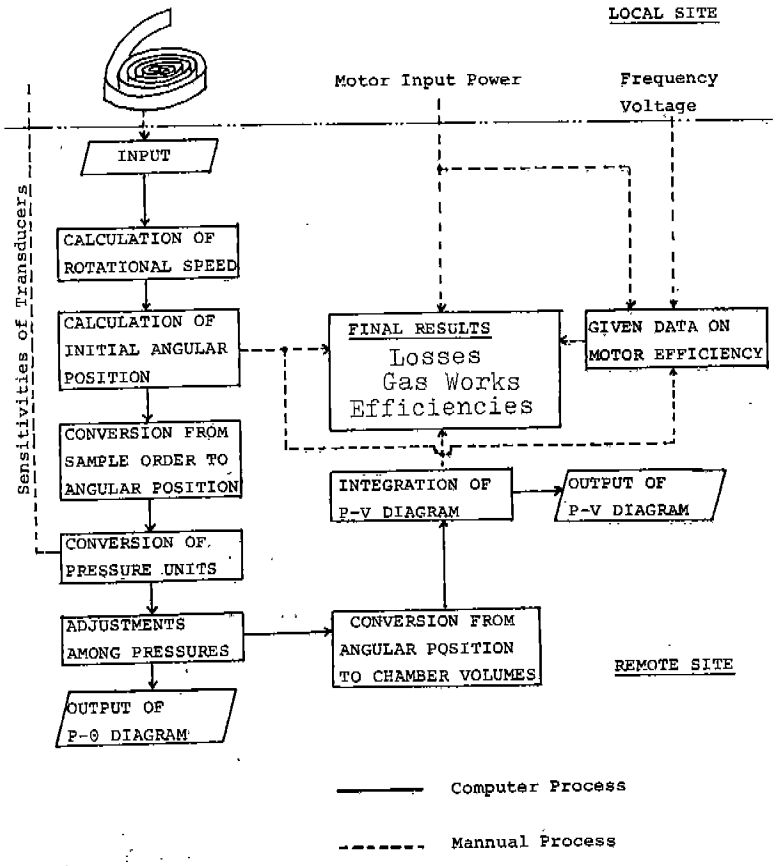

Figure 7 Signal Processing at Remote Site

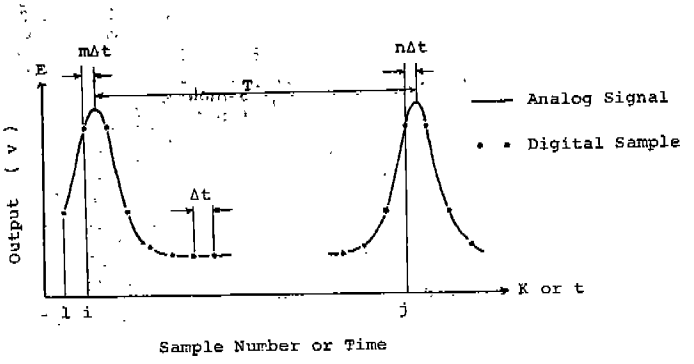

Figure 8 Sampling of Reference Angular Position Signal

Order of Adjustment	Reference Pressure	Pressure Adjusted	Average Range
1	P_e	P_s	306° < θ < 342°
2	P_s	P_M	306° < θ < 342°
3	P_M	P_c	40° < θ < 60°

Table 2 Adjustment of Absolute Pressure Levels

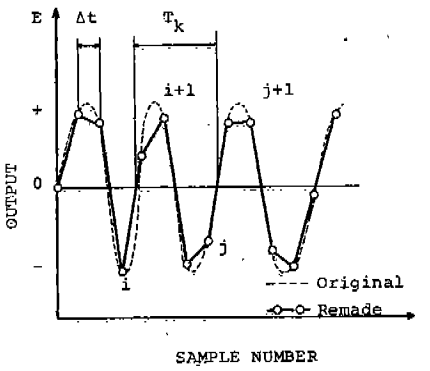

Figure 9 Wave Form of Gear Teeth

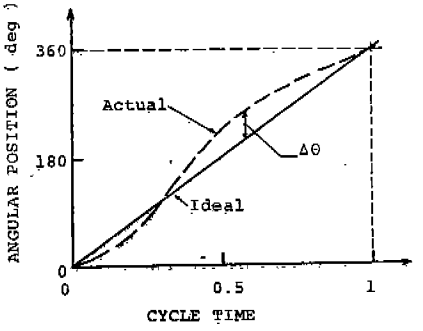

Figure 10 Angular Position Shift

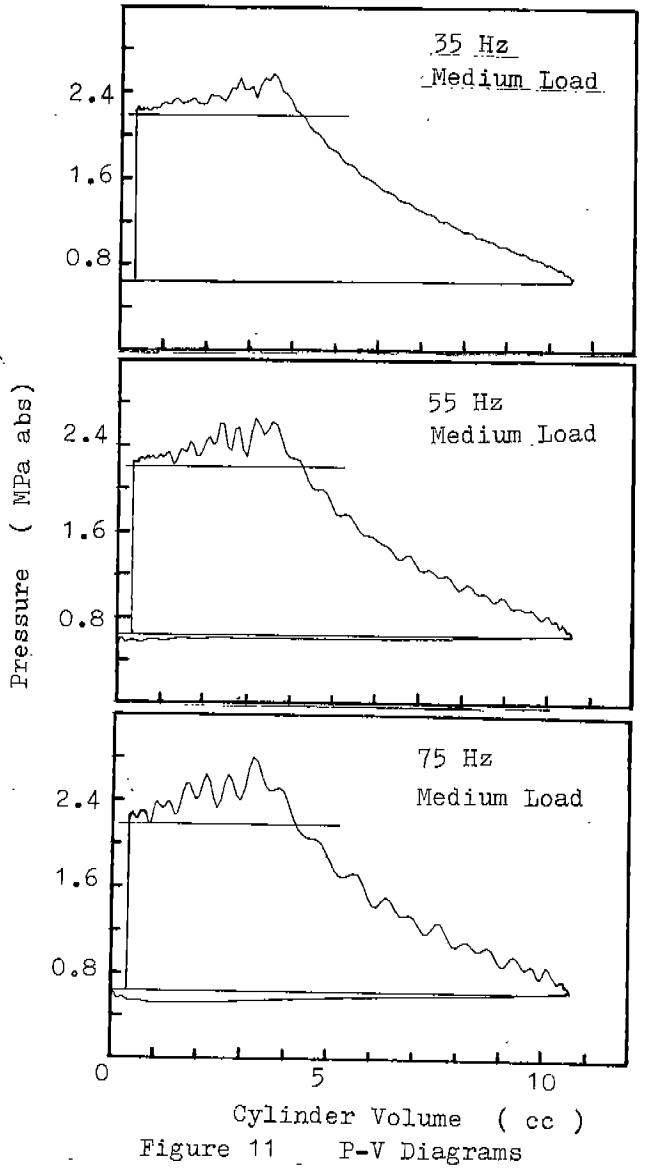

Figure 11 P-V Diagrams

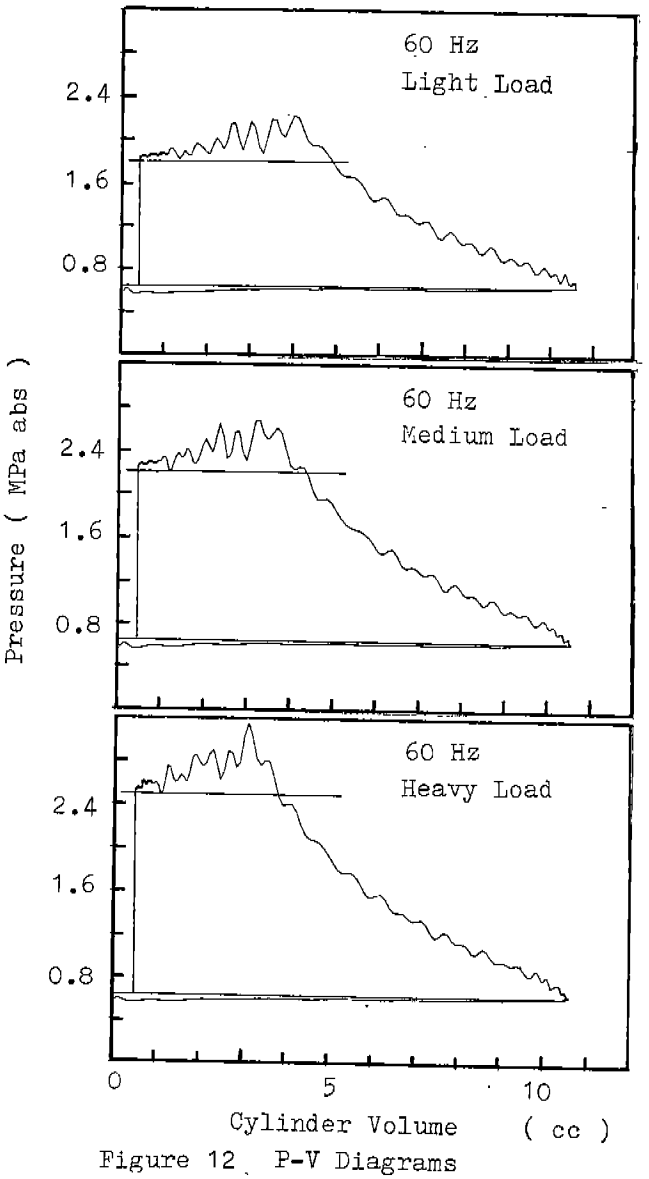

Figure 12 P-V Diagrams

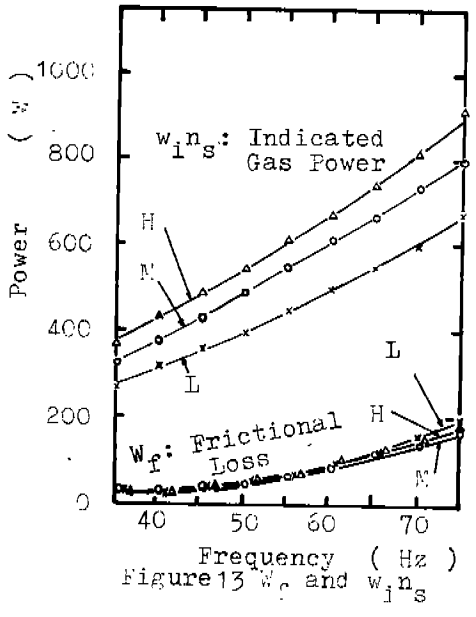

Figure 13 W_f and $w_i n_s$

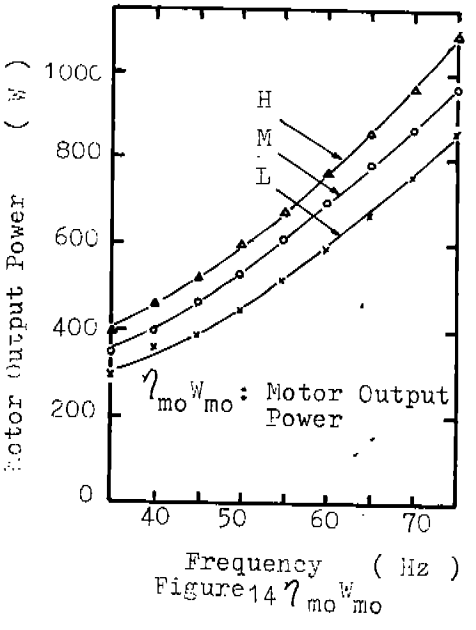

Figure 14 $\eta_{mo} W_{mo}$

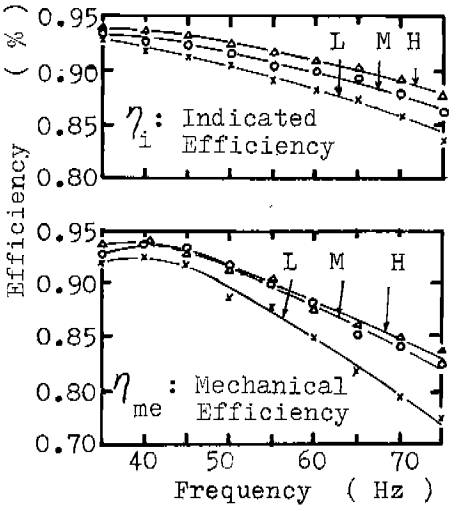

Figure 15 η_i and η_{me}

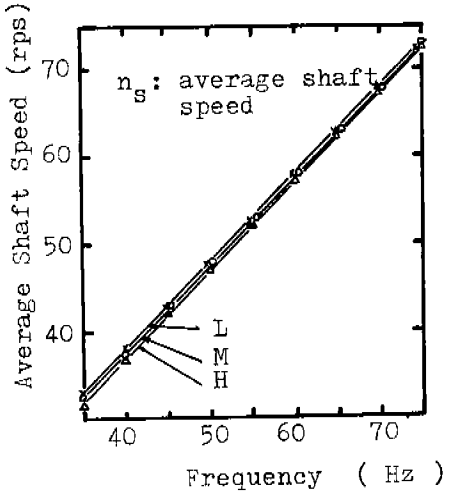

Figure 16 n_s

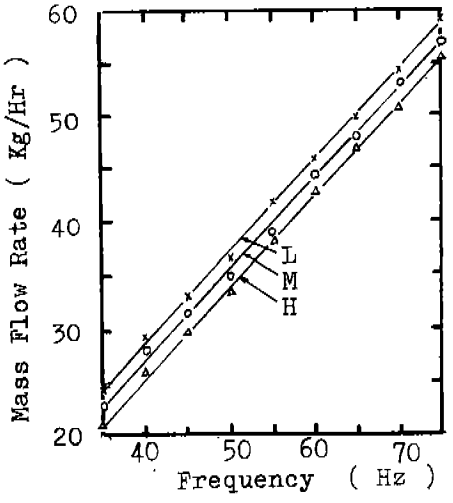

Figure 17 Mass Flow Rate

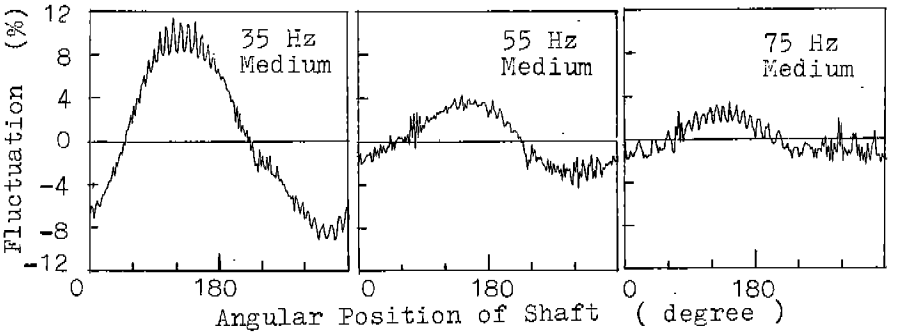

Figure 18 D: Shaft Speed Fluctuation

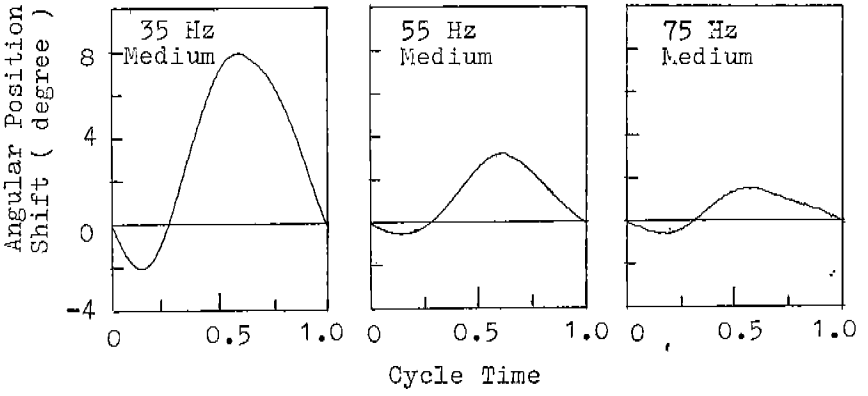

Figure 19 $\Delta\theta$: Angular position Shift

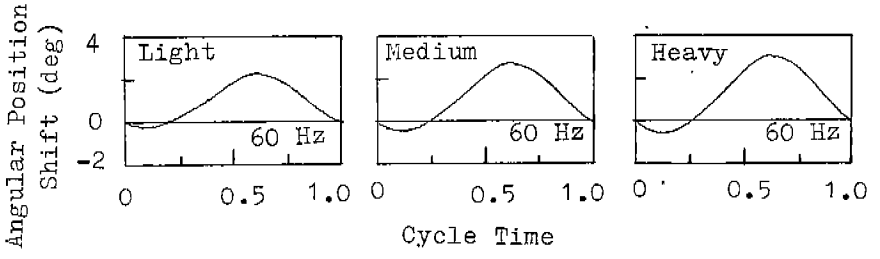

Figure 20 $\Delta\theta$: Angular Position Shift

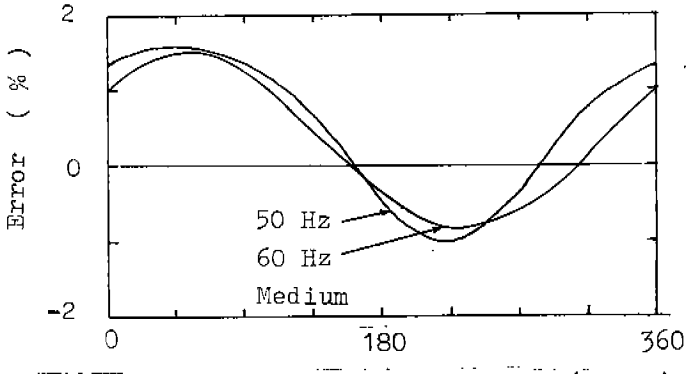

Figure 21 Error of Indicated Gas Work due to Constant Speed Assumption